

Broadband surface-wave transformation cloak

Su Xu^{†1,2}, Hongyi Xu^{†3,4}, Hanhong Gao⁵, Yuyu Jiang^{1,2}, Faxin Yu⁶, John D.

Joannopoulos⁷, Marin Soljačić⁷, Hongsheng Chen^{*1,2,7}, Handong Sun^{*3,4}, and Baile

Zhang^{*3,4}

¹State Key Laboratory of Modern Optical Instrumentation, Zhejiang University, Hangzhou 310027, China

²The Electromagnetics Academy at Zhejiang University, Department of Information Science & Electronic Engineering, Zhejiang University, Hangzhou 310027, China

³Division of Physics and Applied Physics, School of Physical and Mathematical Sciences, Nanyang Technological University, Singapore 637371, Singapore

⁴Centre for Disruptive Photonic Technologies, Nanyang Technological University, Singapore 637371, Singapore

⁵Department of Electrical Engineering and Computer Science, Massachusetts Institute of Technology, Cambridge, MA 02139, United States

⁶School of Aeronautics and Astronautics, Zhejiang University, Hangzhou 310027, China

⁷Research Laboratory of Electronics, Massachusetts Institute of Technology, Cambridge, MA 02139, United States.

[†]These two authors contributed equally to the work.

*Authors to whom correspondence should be addressed; E-mail: hansomchen@zju.edu.cn (H. Chen); hdsun@ntu.edu.sg (H. Sun); blzhang@ntu.edu.sg (B. Zhang)

The ability to guide surface electromagnetic (EM) waves around sharp corners and other types of disorder, without disturbing the wave amplitude or phase, is in great demand for modern photonic and plasmonic devices^{1,2}. This is fundamentally difficult to realize because light momentum must be conserved in a scattering event. A partial realization has been achieved by exploiting topological EM surface states³⁻⁷, but this approach is limited to narrow-band light transmission and subject to phase disturbances in the presence of a corner or disorder⁸. Recent advances in transformation optics^{9,10} apply principles of general relativity to curve the space for light, allowing one to match the momentum and phase of light around any disorder, as if that disorder were not there. This feature has been exploited in the development of invisibility cloaks¹¹⁻¹⁹. An ideal invisibility cloak, however, would require the phase velocity of light being guided around the "cloaked object" to exceed the vacuum speed of light – a feat potentially achievable only over an extremely narrow band^{10,11,20}. In this work we theoretically and experimentally demonstrate that the bottlenecks encountered in previous studies can be overcome. We introduce a new class of cloaks capable of remarkable broadband surface EM waves guidance around ultra-sharp corners and bumps with no perceptible changes in amplitude and phase. These cloaks consist of specifically designed non-magnetic metamaterials, and they achieve nearly ideal transmission efficiency over a broadband frequency range from 0+ to 6 GHz. This work provides strong support for the application of transformation optics to plasmonic circuits, and could pave the way towards high performance, large-scale integrated photonic circuits.

One of the main limitations in plasmonic circuitry and devices^{1,2} that utilize surface EM waves (surface plasmons at optical frequencies) as information and energy carriers is the inability to perfectly guide surface EM waves around unavoidable disorders such as sharp corners. While near-perfect transmission around sharp corners in electronic circuits is routine, it is fundamentally difficult to realize with surface waves because surface waves suffer from scattering loss when encountering sharp corners or other irregular disorders.

“Scattering-free” guidance of surface waves around sharp corners has been demonstrated only in topological EM surface states³⁻⁶. It has been developed in analogy with electronic chiral edge states in quantum Hall systems²¹ and with topological insulators^{22,23}. In order to force the waves to circumvent disorders, the studies cited above typically require the use of photonic crystals with substantial magnetic responses. The use of magnetic metamaterials limits these realizations to a narrow microwave frequency band. The use of conventional nonmagnetic photonic materials, on the other hand, could allow for scalability to the optical regime with broad bandwidth.

The difficulty in sharp bending is the dramatic momentum mismatch of surface EM waves before and after passing the sharp corner in an extremely compact space. Transformation optics^{9,10} allows for the design of inhomogeneous metamaterials that control light by effectively warping the EM space analogously to the way gravity curves space in general relativity. Since the concept of momentum stems essentially from space homogeneity²⁴, an effectively curved EM space provides a method to match wave momenta by compensating for the asymmetry of spatial translation around sharp corners. Surface EM waves can be thereby deceived as if they were still propagating along a flat surface, without any corners.

In the past few years, transformation optics has been used to develop invisibility cloaks to hide objects from free-space propagating EM waves¹¹⁻¹⁹. However, an ideal invisibility cloak is fundamentally narrow band because it would require the phase velocity of light being guided around the “cloaked object” to exceed the vacuum speed of light^{10,11,20}. On the other hand, surface EM waves are essentially “slow” waves, whose bending will not cause superluminal propagation in the majority of situations. Yet all of the potential applications of transformation optics in surface EM waves²⁵⁻²⁹ so far are still theoretical. Most theoretical designs only dealt with objects with relatively smooth surfaces or finite bending radii^{25,26}. Refs. 28 and 29 proposed alternative surface wave bending approaches; yet in general scattering will occur when an ultra-sharp bending with zero radius is desired. Therefore, if a similar approach of sharp bending could be realized for surface waves, many unique conceivable applications would become feasible: not only waveguides for sharp right-angle corners³, but also carpet cloaks that can hide irregular bumps on the metal/dielectric interface²⁶, super plasmonic resonators with extremely high Q values³⁰, etc.

Here we present experimental demonstration of broadband sharp bending of surface EM waves with almost ideal transmission; this allows “invisibility cloaking” of disorders such as ultra-sharp corners and bumps for surface EM waves. The remarkable broadband guidance, lacking in previous “scattering-free” topological EM surface states and free-space invisibility cloaks, is because of two reasons. Firstly, the “slow wave” property of surface EM waves can overcome the bottleneck of free-space invisibility cloaks since its phase velocity does not need to exceed the vacuum speed of light. Secondly, we adopt a fully non-magnetic design with naturally accessible dielectric parameters, while magnetic responses were necessary to open the topological band gap for topological EM surface states.

We start with the demonstration of bending a surface EM wave across sharp right-angle corners at microwave frequencies—similar to the previous demonstration of bending a guided topological surface EM wave in a photonic crystal³. We call the bending adaptor a “corner cloak,” as it effectively hides a corner to the wave as if the corner did not exist. Since metals at microwave frequencies are perfect electric conductors that generally do not support surface EM waves, here we adopt the approach of geometrically-induced, or “spoof,” surface plasmons³¹—i.e., we use a grooved metallic surface (referred to as a “patterned metal” in Figs. 1, 2, 3) to support surface EM waves in the microwave regime. Fig. 1a shows the experimental setup: a U-shaped surface-wave waveguide (a metal base with periodic grooves on its surfaces: i.e., the patterned metal) with two right-angle zero-radius corners. Given the sizes of the cloaks, the more confined the surface waves on the dielectric-metal interface, the better the cloaking performance. To enhance the confinement, we load the grooves with ceramic material with permittivity $\epsilon_{ceramic}=21$. We use glass with permittivity $\epsilon_b=4.6$ as the surrounding background that is to be impedance-matched with the cloaks. More details can be found in the Supplementary Information.

The two identical corner cloaks locate at the two corners. This structure that consists of the U-shaped waveguide and two corner cloaks can be thought of as if it were transformed from a straight waveguide without any corner. A corner cloak, when transformed back, corresponds to a triangular space on top of the dielectric-metal interface, whose area is purposely chosen to be the same as the corner cloak. This area preservation guarantees non-magnetism in the cloak design for surface EM waves. (See Supplementary Information for more details.) The two identical corner cloaks require anisotropic constitutive parameters. For each cloak the required principal permittivities in two orthogonal directions, ϵ_1 and ϵ_2 , after the procedure of

diagonalization, where only components in the xy -plane are relevant, are $\varepsilon_1=10.7$ and $\varepsilon_2=2.0$. These cloaks were implemented with a metamaterial consisting of a stack of the following two materials with subwavelength thickness: a microwave dielectric ceramic with permittivity $\varepsilon_{ceramic}=21$ (Wuxichaoying[®] K-21; loss tangent: 1×10^{-4} ; 1 mm thickness) and a polymer foam with permittivity $\varepsilon_{foam}=1.1$ (Rohacell[®] 71HF; loss tangent: 16×10^{-4} ; 1.06 mm thickness). According to the standard formulae of effective medium theory, one can get

$$\begin{cases} \varepsilon_1 = r\varepsilon_{ceramic} + (1-r)\varepsilon_{foam} \\ \varepsilon_2 = \varepsilon_{ceramic}\varepsilon_{foam} / [(1-r)\varepsilon_{ceramic} + r\varepsilon_{foam}] \end{cases},$$

where the filling factor is given by $r=0.485$. Fig. 1b shows the simulation of the transmission of surface EM waves when the corners are *not* cloaked by the corner cloaks; a dramatic scattering loss is evident. However, the transmission of surface EM wave across a sharp corner is perfect when both corners are cloaked by corner cloaks (Fig. 1c).

A fabricated model with two corner cloaks is shown in Fig. 1d. For comparison, we also fabricated a straight waveguide (not shown here) with similar grooves and the same total propagation distance. The transmission data measured on the U-shaped surface-wave waveguide from 0^+ (100 MHz) to 6 GHz without/with corner cloaks are normalized to the transmission data measured on the straight waveguide (Fig. 1e). Without corner cloaks, the transmission measured at the output of the U-shaped waveguide is close to zero, but when both sharp corners are hidden by the corner cloaks, the transmission is almost unity. This shows near-perfect cloaking of two right-angle zero-radius corners for surface EM waves in a broad bandwidth from 0^+ to 6 GHz, i.e. with a fractional bandwidth of 200%.

Next we demonstrate a surface-wave carpet cloak used to cover an ultra-sharp

bump on a flat metal/dielectric interface. Fig. 2a shows our experimental setup. As in the realization of the corner cloaks, we used a metal base with grooves to support surface EM waves. A sharp bump on the flat surface acts as an obstacle able to block the propagation of surface EM waves. The carpet cloak that can hide this sharp bump was designed with a similar transformation-optics approach. The numerical simulation for the real structure in the presence of a sharp bump is shown in Fig. 2b and 2c: without a carpet cloak, most of the wave energy is scattered into the background medium near the apex of the bump; when the carpet cloak is put on top of the bump, however, the EM surface waves can be smoothly guided around the bump and return to their original path as if the bump were not there. A fabricated model with a carpet cloak implemented with the same metamaterial used in the corner cloaks is shown in Fig. 2d. The measured transmissions, normalized to the transmission through a straight waveguide without the bump, are shown in Fig. 2e. For the setup without a cloak, the normalized transmission is close to zero, indicating that the propagation of surface EM waves has been blocked by the bump. For the case with a carpet cloak, the normalized transmission approaches unity, showing near-perfect cloaking of a sharp bump for surface EM waves in a broad bandwidth from 0⁺ to 6 GHz.

A striking feature, absent in topological EM surface states, is that when the surface waves are perfectly guided by the cloaks, the phase is preserved. We used a pulsed signal to demonstrate this behavior. Fig. 3 shows the dynamic propagation of a pulse through the cloaks, obtained with the commercial software COMSOL Multiphysics. A point source at Port 1 excites a Gaussian shaped pulse (bandwidth: 0⁺ to 6 GHz; center frequency: 3 GHz) at 0 ns. The magnetic field distributions are plotted to show the propagation of the pulse on the patterned metal for the setup with

the corner cloaks (Fig. 3a), the carpet cloak (Fig. 3b), and a straight waveguide as a reference (Fig. 3c). For the realization with corner cloaks, the signal reaches the first and the second sharp corners at 1.88 ns and 3.56 ns, respectively. At both sharp corners, the pulse signal is perfectly guided by the corner cloak and at last it leaves the patterned metal from Port 2. In the case of the carpet cloak, the pulse reaches the bump at 2.68 ns and it is guided smoothly across the bump by the carpet cloak without any loss. The pulse reaches the same positions as in the straight waveguide, with no relative delay, indicating that the phase is well preserved in a broad bandwidth by the cloaks. Two videos with more details of the propagating pulse are included in the Supplementary Information. Fig. 4a and 4b show the measured phase for the corner cloak and carpet cloak, respectively. The curves almost coincide with their references over the frequency band from 0⁺ to 6 GHz, confirming that the phase of the surface wave is well preserved by the cloaks.

The above results demonstrate “scattering-free” guidance of surface EM waves around large disorders with both wave energy and phase undisturbed in a 200% broad frequency band. Switching from free-space EM waves to surface EM waves, transformation cloaks can find immediate applications without any fundamental limitations. The fully non-magnetic design makes it feasible to further extend to higher frequencies and/or to conventional surface waves. Our work thereby paves the way towards the next-generation of photonic and plasmonic devices, allowing for flexible design without concern in disorders.

Supplementary Information is linked to the online version of the paper at <http://www.pnas.org>.

Acknowledgements We thank P. Rebusco for critical reading and editing of the manuscript. We thank Y. Deng for fabricating the samples. This work was sponsored by the NNSFC (Grants Nos. 61322501 and 61275183), the National Top-Notch Young Professionals Program, the FANEDDC-200950, the NCET-12-0489, the FRFCU-2014XZZX003-24, NTU-NAP Start-Up Grant, and Singapore Ministry of Education under Grant No. Tier 1 RG27/12 and MOE2011-T3-1-005. The work at MIT was supported by the U. S. Army Research Laboratory and the U. S. Army Research Office through the Institute for Soldier Nanotechnologies, under contract number W911NF-13-D-0001, and M. S. was supported in part by the MIT S3TEC EFRC of DOE under Grant No. de-sc0001299.

Author contributions All authors contributed extensively to this work. B.Z. conceived the idea of the study. S.X. conducted experiment and analysis. H.X., and S.X. performed the numerical simulations. H.X and H.G. designed the cloaking and groove structure. Y.J. and F.Y. provided the technical contributions to the experiment. H.C., H.S. and B.Z. supervised the project. H.C. coordinated the efforts of the research team and directed the experiments. S.X., H.X., J.D.J., M.S, H.C., H.S and B.Z. analyzed data, discussed and interpreted detailed results, and wrote the manuscript with input from all authors.

Author Information Reprints and permissions information is available at www.pnas.org. The authors declare no competing financial interests. Readers are welcome to comment on the online version of the paper. Correspondence and requests

for materials should be addressed to H.C. (hansomchen@zju.edu.cn), H.S. (hdsun@ntu.edu.sg), or B.Z. (blzhang@ntu.edu.sg).

References

1. Raether H (1988). *Surface Plasmons on Smooth and Rough Surfaces and on Gratings* (Springer-Verlag, New York).
2. Ozbay E (2006) Plasmonics: Merging photonics and electronics at nanoscale dimensions. *Science* 311(5758): 189-193.
3. Wang Z, Chong Y, Joannopoulos JD, Soljacic M (2009) Observation of unidirectional backscattering-immune topological electromagnetic states. *Nature* 461(7265): 772-775.
4. Lu L, Joannopoulos JD, Soljacic M (2014) Topological photonics. *Nat Photonics* 8(11): 821-829.
5. Khanikaev AB, et al. (2013) Photonic topological insulators. *Nat Mater* 12(3): 233-239.
6. Chen W-J, et al. (2014) Experimental realization of photonic topological insulator in a uniaxial metacrystal waveguide. *Nat Commun* 5: 5782.
7. Fang K, Yu Z, Fan S (2012) Realizing effective magnetic field for photons by controlling the phase of dynamic modulation. *Nat Photonics* 6(11): 782-787.
8. Wang Z, Chong YD, Joannopoulos JD, Soljacic M (2008) Reflection-free one-way edge modes in a gyromagnetic photonic crystal. *Phys Rev Lett* 100(1): 013905.
9. Leonhardt U (2006) Optical conformal mapping. *Science* 312(5781): 1777-1780.
10. Pendry JB, Schurig D, Smith DR (2006) Controlling electromagnetic fields. *Science* 312(5781): 1780-1782.
11. Schurig D, et al. (2006) Metamaterial electromagnetic cloak at microwave frequencies. *Science* 314(5801): 977-980.
12. Liu R, et al. (2009) Broadband ground-plane cloak. *Science* 323(5912): 366-369.
13. Valentine J, Zentgraf J, Li T, Bartal G, Zhang X (2009) An Optical cloak made of dielectrics. *Nat Mater* 8(7): 568-571.
14. Gabrielli LH, Cardenas J, Poitras CB, Lipson M (2009) Silicon nanostructure cloak operating at optical frequencies. *Nat Photonics* 3(8): 461-463.
15. Ergin T, Stenger N, Brenner P, Pendry JB, Wegener M (2010) Three-dimensional invisibility cloak at optical wavelengths. *Science* 328(5976): 337-339.
16. Ma HF, Cui TJ (2010) Three-dimensional broadband ground-plane cloak made of metamaterials. *Nat Commun* 1: 21.
17. Zhang B, Luo Y, Liu X, Barbastathis G (2011) Macroscopic invisibility cloak for visible light. *Phys Rev Lett* 106(3): 033901.
18. Chen X, et al. (2011) Macroscopic invisibility cloaking of visible light. *Nat Commun* 2: 1176.
19. Landy N, Smith DR (2013) A full-parameter unidirectional metamaterial cloak for microwaves. *Nat Mater* 12(1): 25-28.
20. Chen H, et al. (2013) Ray-optics cloaking devices for large objects in incoherent natural light. *Nat Commun* 4: 2652.
21. Klitzing KV (1986) The quantized Hall effect. *Rev Mod Phys* 58(3): 519-531.
22. Hasan MZ, Kane CL (2010) Colloquium: topological insulators. *Rev Mod Phys* 82(4): 3045-3067.
23. Qi XL, Zhang SC (2011) Topological insulators and superconductors. *Rev Mod Phys* 83(4): 1057-1110.
24. Landau LD, Lifshitz EM (1969) *Mechanics* (Pergamon Press, Oxford, ed.2).
25. Burkay D, Teixeira FL (2008) Metamaterial blueprints for reflectionless waveguide bends. *IEEE Microw Wirel Co* 18(4): 233-235.
26. Liu Y, Zentgraf T, Bartal G, Zhang X (2010) Transformational plasmon optics. *Nano Lett* 10(6): 1991-1997.
27. Zhang J, Xiao S, Wubs M, Mortensen NA (2011) Surface plasmon wave adapter designed with transformation optics. *ACS Nano* 5(6): 4359-4364.
28. Mitchell-Thomas RC, McManus TM, Quevedo-Teruel O, Horsley SAR, Hao Y (2013) Perfect surface wave cloaks. *Phys Rev Lett* 111(21): 213901.
29. Patel AM, Grbic A (2014) Transformation Electromagnetics Devices Based on Printed-Circuit Tensor Impedance Surfaces. *IEEE T Microw Theory* 62(5): 1102-1111.
30. Xu H, Wang X, Yu T, Sun H, Zhang B (2012) Radiation-suppressed plasmonic open resonators designed by nonmagnetic transformation optics. *Sci Rep* 2: 784.
31. Pendry JB, Martín-Moreno L, García-Vidal FJ (2004) Mimicking surface plasmons with structured surfaces. *Science* 305(5685): 847-848.

Figure Legends

Figure 1 | Surface-wave bending around sharp corners. **a**, A U-shaped surface-wave waveguide with grooves on its surface, covered by glass, is illuminated by a dipole antenna. The two sharp corners are covered by two corner cloaks, i.e. layered structures with subwavelength foam and ceramic materials. A second dipole antenna located at the output of the waveguide measures the transmission. **b**, Simulation of a surface wave when it encounters a sharp corner not covered by a cloak. **c**, Simulation of a surface wave when the sharp corner is cloaked by a corner cloak. **d**, Photo of a fabricated model. The transmitter, which is shielded by the microwave absorber material, is not shown in the figure. **e**, Measured normalized transmission of surface waves through the waveguide.

Figure 2 | Surface-wave carpet cloaking. **a**, A straight surface-wave waveguide with a sharp bump is illuminated by a dipole antenna. The surface of the metal base is grooved similarly to Fig. 1a. The sharp bump is covered by a carpet cloak, i.e. a layered structure with subwavelength foam and ceramic materials. A second dipole antenna located at the output of the waveguide measures the transmission. **b**, Simulation of a surface wave when it encounters the sharp bump without a carpet cloak. **c**, Simulation of a surface wave when the sharp bump is cloaked by the carpet cloak. **d**, Photo of a fabricated model. The transmitter, which is shielded by the microwave absorber material, is not shown in the figure. **e**, Measured normalized transmission of surface waves through the waveguide.

Figure 3 | A Gaussian-shaped pulse propagates on the patterned metal. A point source (Port 1) generates the pulse at 0 ns. The bandwidth of the pulse is 6 GHz and the center frequency is 3 GHz. The magnetic field distributions for three cases (the corner cloaks **(a)**, the carpet cloak **(b)**, and the straight waveguide reference **(c)**) are plotted to show the propagation of the pulse at five equivalent temporal sampling points.

Figure 4 | Phase measurements. **a**, The corner cloaks. **b**, The carpet cloak. The phases with the straight waveguide are plotted for reference. In both cases the phase curves almost coincide with their references over the frequency band from 0⁺ to 6 GHz.

Figures

Figure 1

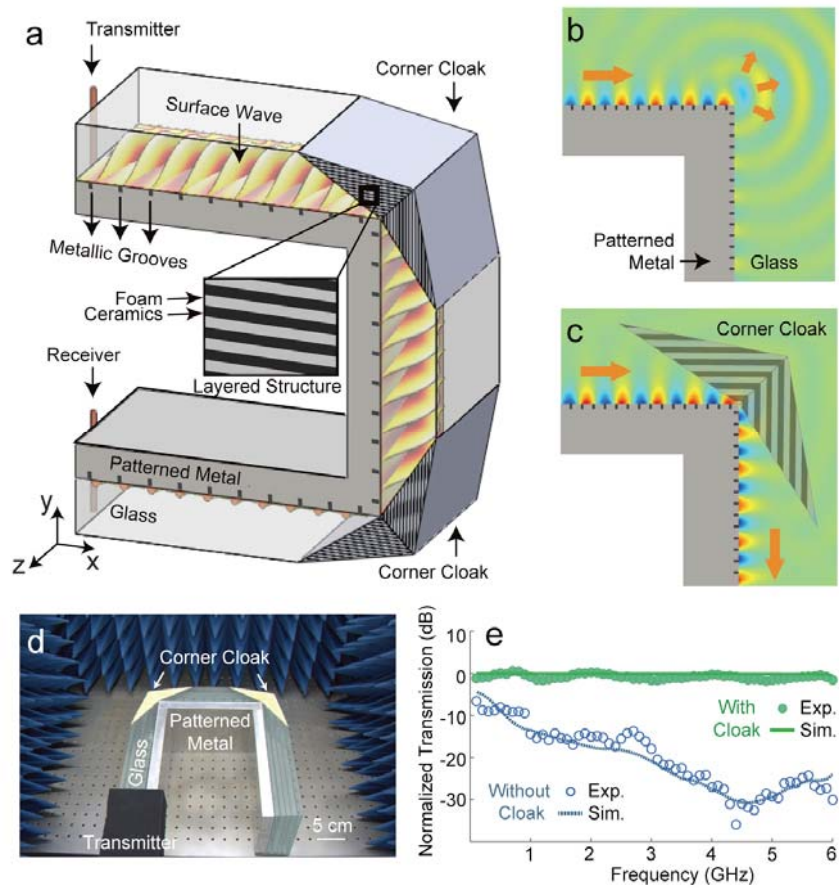


Figure 2

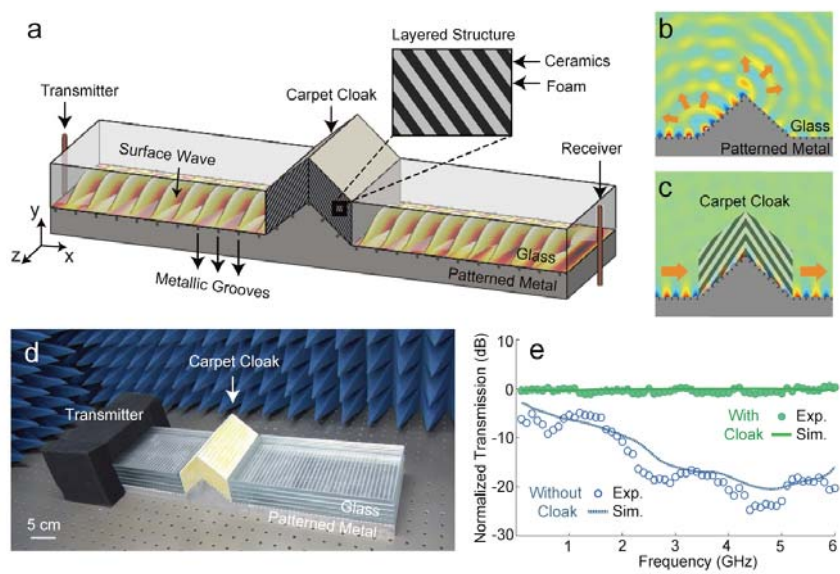


Figure 3

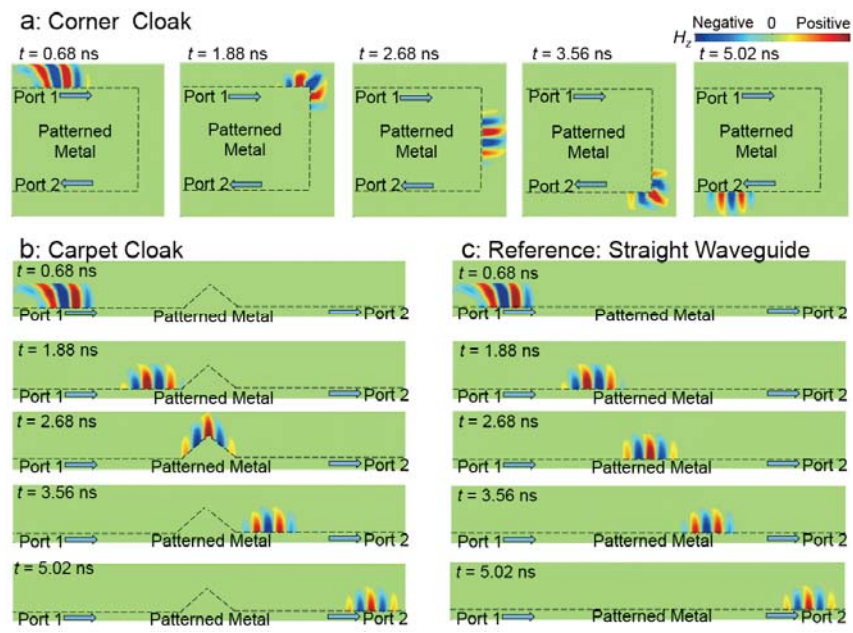
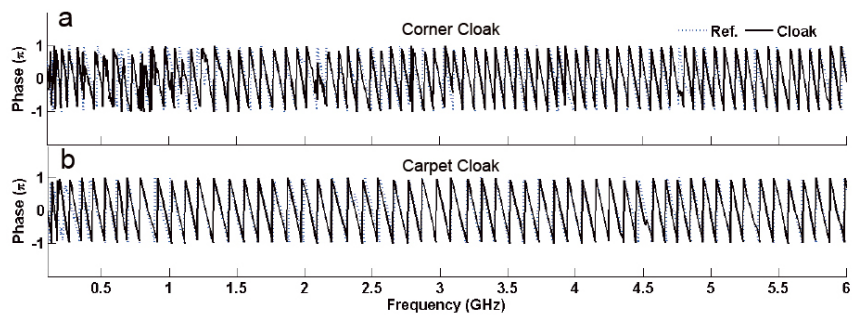


Figure 4



Supplementary Methods

Dispersion relation of spoof surface plasmons on the metallic grooved structure

used in our models. Supplementary Fig. 1a shows the perfect electric conductor (PEC) surface with a 1D periodic array of grooves with periodicity p . Each groove has width w and depth d . All grooves are filled with a ceramic material with permittivity $\epsilon_{ceramic}=21$. The background material above the grooved structure is glass with $\epsilon_b=4.6$. Supplementary Fig. 1b shows the simulated dispersion relation of spoof surface plasmons for $d=2.3$ mm, $w=1.5$ mm and $p=7.5$ mm.

Specifications of the U-shaped waveguide and the corner cloaks.

Here we briefly introduce the transformation design. Supplementary Fig. 2a shows the three-dimensional scheme of the U-shaped waveguide with sharp corners and periodic grooves. The layered metamaterial structure is a stack of Rohacell[®] 71HF foam plates ($\epsilon_{foam}=1.10$; loss tangent 16×10^{-4} ; 1.06 mm thickness) and Wuxichaoying[®] K-21 microwave dielectric ceramic plates ($\epsilon_{ceramic}=21$; loss tangent 1×10^{-4} ; 1 mm thickness). From the effective medium theory, the effective permittivities of the corner cloaks can be obtained as $\epsilon_1=r\epsilon_{ceramic}+(1-r)\epsilon_{foam}$, $\epsilon_2=\epsilon_{ceramic}\epsilon_{foam}/[(1-r)\epsilon_{ceramic}+r\epsilon_{foam}]$, with the filling factor $r=0.485$.

The x - y projection in Supplementary Fig. 2a shows a feasible transformation of the original EM space for EM surface waves propagating on a metal/dielectric interface: the region $M_nO_nA_n$ (blue color) is transformed into $M_nO_nA'_n$ (red color), with its area being preserved; symmetrically, the region $W_nO_nV_n$ is transformed into $W_nO_nV'_n$. The subscript $n=1$ or 2 represents the n th 90° corner. Note that because the surface EM waves have magnetic field along z direction, only the z -component of

permeability is relevant, which, according to the principle of transformation optics, is equal to $\mu_z = 1 / \det(\bar{J})$, where $\det(\bar{J})$ is the Jacobian of the transformation. Since the Jacobian represents the change of an infinitesimal area in the transformation, the area preservation from $M_n O_n A_n$ to $M_n O_n A'_n$ and $W_n O_n V_n$ to $W_n O_n V'_n$ guarantees that $\mu_z = 1$. Thus we can implement a perfect full-parameter metamaterial corner cloak with dielectric materials. For $|A_n O_n| = 50$ mm, $|A_n M_n| = 75$ mm, and $|A'_n O_n| = 42.4$ mm, the required principal permittivities of the corner cloaks are $\varepsilon_1 = 10.7$ and $\varepsilon_2 = 2.0$. Supplementary Fig. 2b shows triangular pieces of the metamaterial structure. Four identical triangles of the metamaterial structure form two corner cloaks that effectively bend surface waves across the two right-angle zero-radius corners of the U-shaped waveguide.

Specifications of the carpet cloak. Supplementary Fig. 3a illustrates the three dimensional scheme of the carpet cloak and the grooved surface-wave waveguide with a sharp bump. The carpet cloak is constructed with a layered metamaterial structure composed of Wuxichaoying[®] K-21 microwave dielectric ceramic plates ($\varepsilon_{ceramic} = 21$; loss tangent 1×10^{-4} ; 1 mm thickness) and Rohacell[®] 71HF foam plates ($\varepsilon_{foam} = 1.10$; loss tangent 16×10^{-4} ; 1.06 mm thickness).

The x - y projection in Supplementary Fig. 3a shows the area-preserving transformation for the carpet cloak. The original rectangular space $HIJK$ (blue color) is transformed into two symmetric and connected parallelograms $HMNK$ and $IMNJ$ (red color), under the area-preservation constraint. The constitutive parameters of the transformation medium are obtained with the same method used for the corner cloaks. Because the area is invariant in the transformation, the permeability is intrinsically unitary. For $|HI| = 100$ mm, $|HM| = 66.6$ mm, and $|HK| = 50$ mm, the carpet cloak

requires the same metamaterial used for the corner cloaks. Supplementary Fig. 3b shows details of the ceramic/foam layered metamaterial structure.

Supplementary Videos

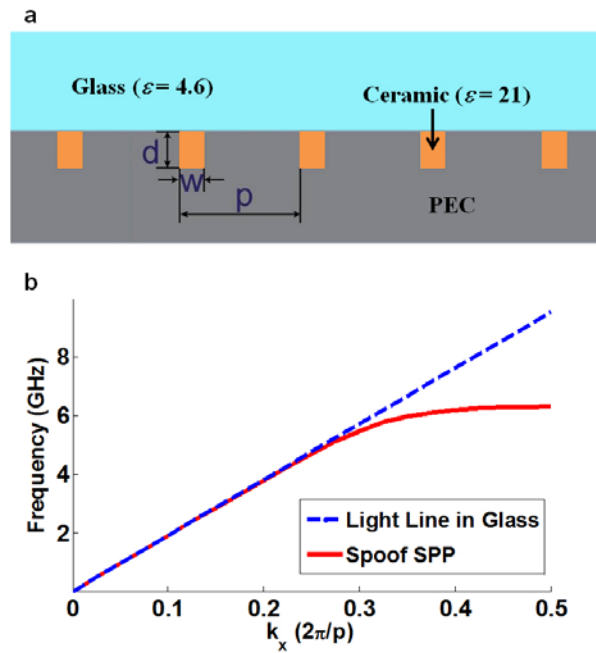
Supplementary Video 1 | A Gaussian-shaped pulse propagates on the patterned

metal with two zero-radius sharp corners. Upper left panel: When there is no cloak, most pulse energy is scattered at the corners. Upper right panel: When two corners are cloaked, the pulse can be perfectly guided around the two sharp corners. Lower panel: A pulse propagates on a straight patterned metal as a reference.

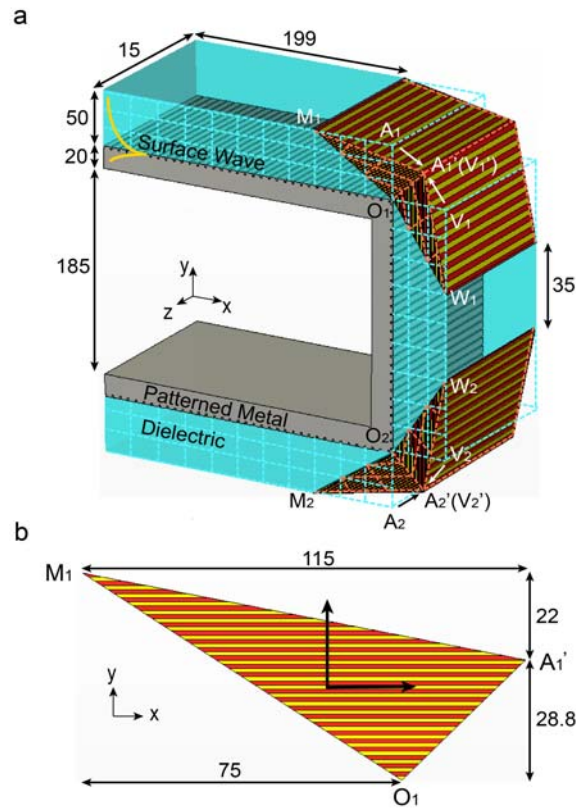
Supplementary Video 2 | A Gaussian-shaped pulse propagates on the patterned

metal with a sharp bump. Upper panel: When there is no cloak, most pulse energy is scattered at the bump. Middle panel: When the carpet cloak hides the bump, the pulse can be perfectly guided around the bump. Lower panel: A pulse propagates on a straight patterned metal as a reference.

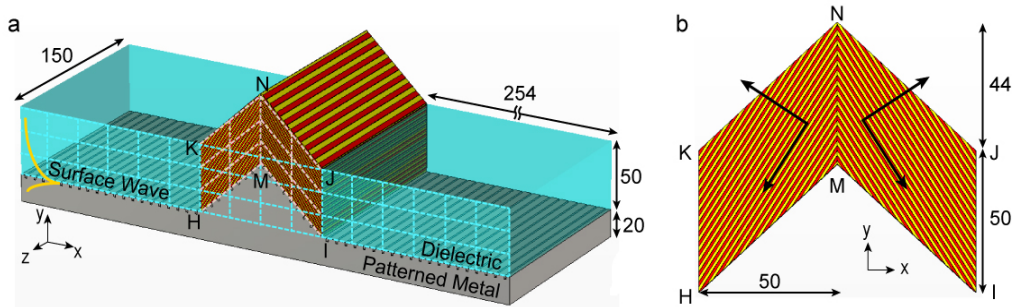
Supplementary Figures



Supplementary Figure 1 | Dispersion relation of spoof surface plasmons on the metallic grooved structure. **a**, Schematic diagram of the metallic grooves. **b**, Dispersion relation of spoof surface plasmons for $d = 2.3$ mm, $w = 1.5$ mm and $p = 7.5$ mm.



Supplementary Figure 2 | Design of the transformation-optics corner cloaks for sharp bending of electromagnetic surface waves. **a**, Three dimensional scheme of the U-shaped surface-wave waveguide. The materials in red, yellow and blue are the microwave ceramic, the dielectric foam, and the low-loss glass, respectively. The areas of the regions $M_nO_nA_n$ and $W_nO_nV_n$ (before the transformation) are preserved over the transformation to $M_nO_nA'_n$ and $W_nO_nV'_n$ respectively, where the subscript n indicates the n th sharp corner. The mesh shows the electromagnetic space above the metal/dielectric interface, while the electromagnetic space below the interface is neglected because of the shallow field penetration in metal. **b**, Dimensions of the ceramic/foam layered metamaterial structure. Four triangles of the metamaterial structure form two corner cloaks. All the dimensions in Supplementary Fig. 2 are in millimeters.



Supplementary Figure 3 | Design of the transformation-optics carpet cloak that hides a sharp bump. **a**, Three dimensional scheme of the carpet cloak and the grooved metallic base with a sharp bump. The materials in red, yellow and blue are the microwave ceramic, the dielectric foam and the low-loss glass, respectively. The area of the region $HIJK$ (before the transformation) is preserved over the transformation to $HMIJNK$. The mesh indicates the electromagnetic space above the metal/dielectric interface, while the electromagnetic space below the interface is neglected because of the shallow field penetration in metal. **b**, Details of the ceramic/foam layered metamaterial structure forming the carpet cloak. All the dimensions in Supplementary Fig. 3 are in millimeters.